Numerical simulation of two-phase non-Newtonian fluid flow inside a microchannel

Amir Haghighatkha
Master of Mechanical Engineering
Tehran, Iran
haghighatkhah.eng@gmail.com

Milad Abdollahi Kahriz
Tehran, Iran
Miladmak@yahoo.com

***Abstract*— in this research, the two-phase non-Newtonian fluid flow inside the micro channel is investigated numerically. For this purpose, the finite volume method has been used. The micro channel studied in this research is based on a 100 mm × 60 mm × 20 mm plate made of polymethyl methacrylate (PMMA). Its cross section is rectangular. A corresponding model for the transition of flow patterns is established, based on several parameters such as the Weber number, the size of the micro channel, the physical properties of fluids, and the surface roughness. Four major flow patterns are observed for cyclohexane-CMC aqueous solutions two-phase flow in rectangular micro channels: droplet flow, slug flow, parallel flow and jet flow. It is found that the larger the concentration of CMC solutions and the smaller the micro channel, the wider of the regions are for the droplet flow and parallel flow.**

Keywords*— *Non-Newtonian fluid, two phase flow, finite volume method, microchannel.

I. INTRODUCTION

Non-Newtonian fluids such as grease, paint, milk, toothpaste and blood are abundant in our daily lives and are widely used in chemical engineering, biochemical engineering, food processing, oil exploration and medical engineering [1-5]. Micro chemical engineering is an emerging technology that has many potentials in emulsification, bioengineering, pharmaceuticals and food engineering [6-9]. However, studies on non-Newtonian fluids in micro chemical engineering are in their infancy. Therefore, the study of non-Newtonian or Newtonian biphasic fluid flow inside micro channels is very important [10-13]. Obviously, the first step is to know the multiphase currents, especially the pattern of multiphase flows inside the micro channels [14]. For example, slug and droplet streams are widely used in the process of chemical synthesis, while parallel streams are widely used in extraction processes [10]. Extensive research has been done on the liquid-liquid biphasic flow pattern for Newtonian fluids. Slug droplet, mono-dispersed droplet, parallel or circular Newtonian fluid flows have been investigated for both circular and rectangular micro channels. The Weber number of continuous and discrete phases are used to construct the flow pattern map and predict the flow pattern transfer for the liquid-liquid two-phase flow in the micro channel, respectively [15]. However, much research has been done on the non-Newtonian liquid-liquid two-phase flow pattern in micro channels.

Lee et al. [20] found slug flow, droplet flow and jet flow for non- Newtonian/Newtonian two-phase flow in flow-focusing microfluidic devices, and a polyethylene oxide-glycerol-deionized water mixture was used as the dispersed phase, and mineral oil as the continuous phase. Lee et al. [20] found slug flow, droplet flow and jet flow for non- Newtonian/Newtonian two-phase flow in flow-focusing microfluidic devices, and a polyethylene oxide-glycerol-deionized water mixture was used as the dispersed phase, and mineral oil as the continuous phase. Arratia et al. [22] investigated the effects of fluid elasticity on liquid–liquid two-phase flow in a cross-slot micro channel. For high molecular weight fluids (106 and 107), slugging, dripping, and streaming flow regimes were observed. While for low molecular weight fluids (103, 104 and 105), only dripping and slugging flow regimes were observed. Obviously, the investigation on the flow patterns of liquid–liquid two-phase flow in non-Newtonian fluids is in its infancy.

In this research, the two-phase flow pattern of non-Newtonian and Newtonian fluids in T-shaped micro channels is investigated. The effect of operating conditions such as flow rate for both phases, continuous phase rheological properties and channel dimensions on the flow pattern transfer is investigated.

II. STATEMENT OF THE PROBLEM

The micro channel studied in this research is based on a 100 mm × 60 mm × 20 mm plate made of polymethyl methacrylate (PMMA). Its cross section is rectangular. The dimensions of the different parts of the geometry are shown in Figure (1).

Aqueous solution of cyclohexane and carboxymethylcellulose flows into the micro channel. The dispersed phase, which includes cyclohexane, is injected from the sub-branch, and the continuous phase, which is an aqueous solution of carboxymethylcellulose, is injected into the main part of the channel. The flow is investigated in a stable, two-dimensional state using computational fluid dynamics. Specifically, Ansys Fluent software has been used in this research. The mass flow rate of the dispersed phase flow is in the range of 0 to 200 ml / h and the mass flow rate of the continuous phase flow is 0 to 300 ml / h. Continuous phase capillary number in the range 0.002185 to 0.09270, continuous phase Reynolds number in the range 0.003643 to 17.1528, continuous phase Weber number in the range 7.9605×10^{-6} to 0.9770, discrete phase capillary number in the range 5.5181×10^{-6} to 0.004258, Reynolds number of discrete phase in the range 0.009630 to 80.2537, Weber number of discrete phase in the range 5.3142×10^{-7} to 0.341. Cyclohexane used as a discrete phase is used for different concentrations (0.1%, 0.25% and 0.5% by weight) of carboxymethylcellulose. Aqueous solution of carboxymethylcellulose is a fluid with high viscosity and low elasticity. The rheological properties of the aqueous solution of carboxymethylcellulose used in this study are shown in Figure (2).

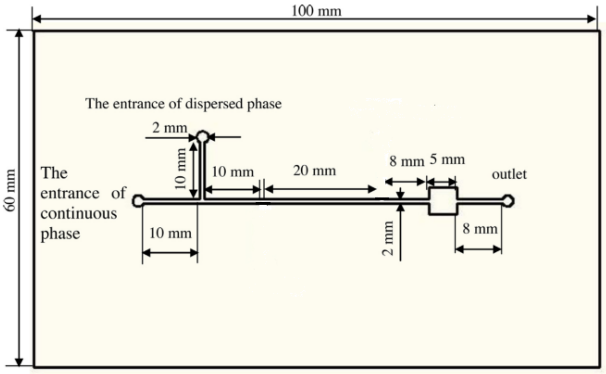

figure 1. Schematic view of the problem under study

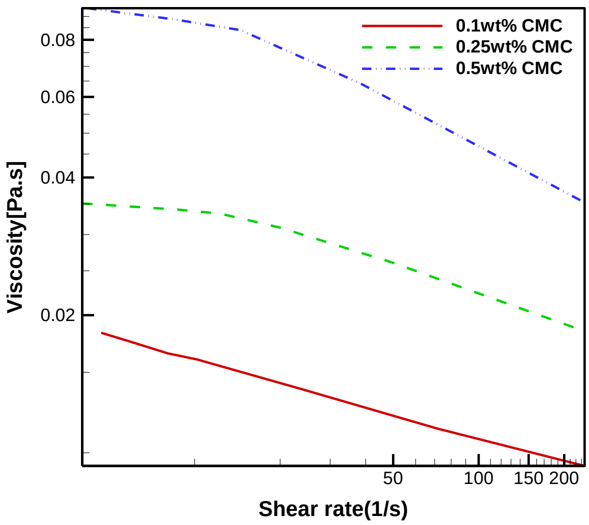

Fig. 2. Rheological properties of non-Newtonian CMC solutions.

As shown in Fig. 2, the CMC aqueous solution is a kind of non-Newtonian fluid with polymer pseudo plastic fluid characteristics. In this paper, the Carreau model [23] is applied to calculate the fluid viscosity:

$$\frac{\mu-\mu_\infty}{\mu_o-\mu_\infty} = [1+(\lambda\dot{\gamma})^2]^{\frac{n-1}{2}} \qquad (1)$$

Where μ_∞ is usually the viscosity of the solvent, so the viscosity of demineralized water is taken to be μ_∞ μ_o is taken as the viscosity of the solvent when its shear rate is zero. λ And n are obtained by using multiple regression method from the rheological data. The various physical parameters of the fluids were gathered in Table 1.

Table 1. Rheological parameters and physical properties of CMC solutions.

fluid	$\rho(\frac{kg}{m^3})$	Liquid-solid Contact angle, $\theta(o)$	Liquid-Liquid Contact angle, $\theta(o)$	$\sigma(\frac{mN}{m})$	Rheological parameter			
					$\mu_o(Pa$	$\mu_\infty(Pa$	$\lambda(s)$	n
Cyclohexane	787	20.3			-	0	-	1
0.2% CMC	1000	75.4	58.5	37.0	0.001	0.001	0.068	0.82
0.25% CMC	1002	81.5	69.4	37.2	0.015	0.001	0.075	0.74
0.5 % CMC	1006	84.1	76.3	38.1	0.096	0.001	0.081	0.64

III. EQUATIONS

In this paper, a two-phase model is used to investigate the flow behavior of non-Newtonian fluid inside the microchannel. The connection equations for the two-phase mixture model are written as follows:

$$\nabla.(\rho_m.\vec{v}_m) = 0 \qquad (2)$$

Mixture density and mixing velocity for n phases are defined as follows:

$$\rho_m = \sum_{k=1}^{n} \varphi_k \rho_k \qquad (3)$$

$$v_m = \frac{1}{\rho_m} \sum_{k=1}^{n} \varphi_k \rho_k \vec{v}_k \qquad (4)$$

In the above relations $\vec{v}_m$ is the mixture velocity and ρ_m is the mixture density.

The momentum equation for the n-phase mixture model is defined as follows:

$$\nabla.\sum_{k=1}^{n} \varphi_k \rho_k \vec{v}_k \vec{v}_k = -\sum_{k=1}^{n} \varphi_k \nabla P_k + \nabla.\sum_{k=1}^{n} \varphi_k (\tau_k + \tau_{Tk}) + \sum_{k=1}^{n} \varphi_k \rho_k \vec{g} \qquad (5)$$

So:

$$\nabla.\sum_{k=1}^{n} \varphi_k \rho_k \vec{v}_k \vec{v}_k = -\nabla.(\rho_m \vec{v}_m \vec{v}_m) + \nabla.\sum_{k=1}^{n} \varphi_k \rho_k \vec{v}_{dr.k} \vec{v}_{dr.k} \qquad (6)$$

For a two-phase mixture

$$\nabla.(\rho_m \vec{v}_m \vec{v}_m) = -\nabla P_m + \nabla.(\tau_k) + \nabla.\tau_{Dm} + \rho_m \vec{g} \qquad (7)$$

In the above relation τ_m and τ_{Dm} are the mean viscous stress and the distribution of slip stress between the two phases, respectively. Stress tensors are defined as follows:

$$\tau_m = \sum_{k=1}^{n} \varphi_k \tau_k \qquad (8)$$

$$\tau_{Dm} = -\sum_{k=1}^{n} \varphi_k \rho_k v_{dr.k} v_{dr.k} \qquad (9)$$

In the above relations $v_{dr.k}$ is the penetration rate of each phase.

For example, the phase velocity k of the mixture velocity is written as follows:

$$v_{dr.k} = v_k - v_m \qquad (10)$$

The energy equation is written as follows:

$$\nabla.\left[\left(\varphi\rho_p C_{p.p}\vec{v}_p\right)+(1-\varphi)\rho_f C_{p.f}\vec{v}_f\right]T=\nabla.(\mathrm{k}\nabla T)+\mu\left(\frac{dv_{m.x}}{dy}\right)^2+Q_o(T-T_b)+\frac{1}{\sigma_{eff}}(\vec{J}.\vec{J})+\rho_p C_{p.p}\left(\frac{D_T}{T}\frac{\partial T}{\partial y}\right)\frac{\partial T}{\partial y} \quad (11)$$

$$\frac{\partial y}{\partial x}\left(\frac{D_T}{T}\frac{\partial T}{\partial y}\right)=0 \quad (12)$$

In the above relations, Q_o ،T ،k ،D_T show the heat source, temperature, thermal conductivity and diffusion coefficient of thermophoresis forces, respectively. In the thermally developed zone $\frac{dT}{dx}=\frac{dT_m}{dx}=\frac{dT_w}{dx}$ because the axial temperature changes are constant, the diffusion term in the x direction is omitted.

Slip velocity (relative velocity) is defined as the secondary phase velocity (p) relative to the initial phase velocity:

$$\vec{v}_{mf}=\vec{v}_p-\vec{v}_f \quad (13)$$

IV. RESULTS AND DISCUSSION

Four major flow patterns are observed for cyclohexane-CMC aqueous solutions two-phase flow in rectangular micro channels as shown in Fig. 3: droplet flow, slug flow, parallel flow and jet flow. A typical flow patterns map is displayed in Fig. 4, with the superficial velocities of the dispersed and continuous phases respectively used as the horizontal and vertical coordinates. Our findings are similar to those of Lee et al. [20] and Arratia et al. [22], and are different from those of Yang et al. [24], Fu et al. [14] and Xu et al. [18], as the annular flow is not observed in our experiments. When the flow rates of both phases are small, the dispersed phase enters into the continuous phase in the form of slug drop, with its length is greater than the channel width, as shown in Fig. 3(a). With increasing the flow rate of the continuous phase Q to a certain value, small disk-liked droplet is formed, with its diameter is smaller than the channel width as shown in Fig. 3(b). When the flow rate of the dispersed phase is increased to a fixed value, the jet flow is formed and the dispersed thread is elongated as shown Fig. 3(c), as the shear force of the continuous phase exerted on the dispersed phase is not high enough to collapse it at the T-junction, but at a position several times of the channel width further from the junction in the downstream micro channel. As the flow rate of the dispersed phase is further increased and the flow rate of the continuous phase is not large enough to collapse the disperse phase into droplets, parallel flow is formed as shown in Fig. 3(d). The continuous phase moves in parallel to the dispersed phase in the micro channel, with a relatively stable liquid–liquid interface. In addition to the above-mentioned major flow patterns, wavy parallel flow, mono-dispersed droplets flow are also observed. These flow patterns are unstable, and are gradually transformed to the main flow patterns.

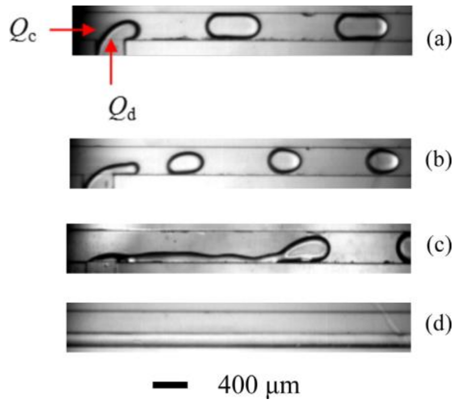

Fig. 3. Representative flow patterns of cyclohexane-CMC two-phase flow in rectangular microchannels. (a) slug flow; (b) droplet flow; (c) jet flow; (d) parallel flow.

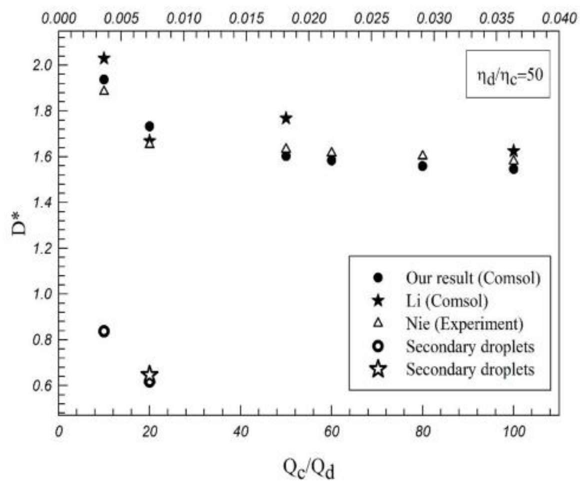

Figure 4. Numerical analysis of simulation results with laboratory results and other numerical results for viscous ratio 50

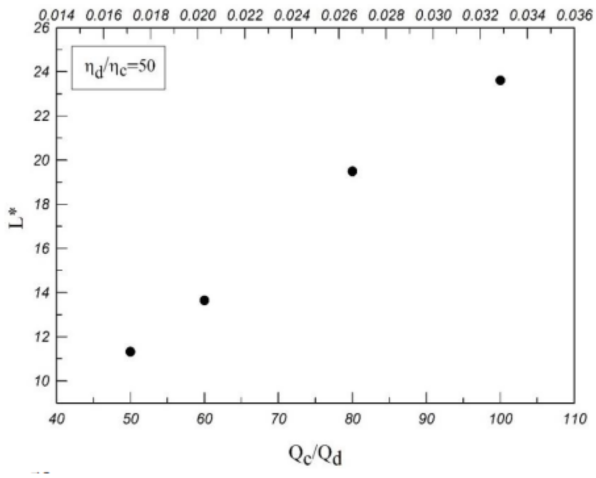

Figure 5. The distance between the droplets in terms of flow rate and different capillaries per viscous ratio is 50

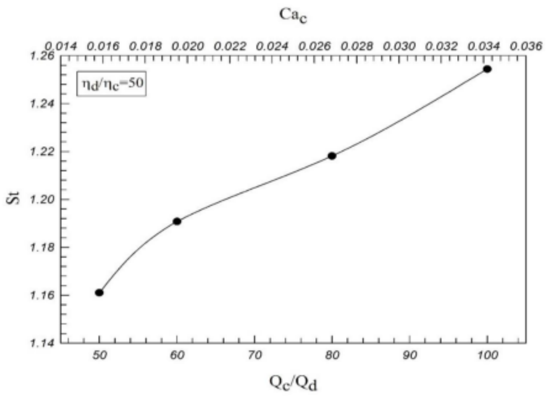

Figure 6. Frequency of droplet production (Strohwell number) in different capillary numbers per viscosity 50

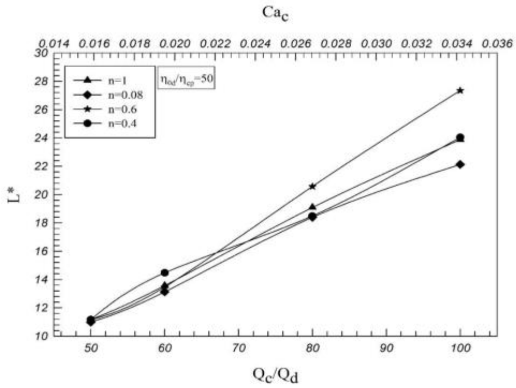

Figure 7. Comparison of distance between droplets in different power indices per 50 viscosity ratio

The fitting results of the transition lines of adjacent flow patterns are shown in Fig. 8. It could be seen that all the experimental points fall into in a straight line for the transition of adjacent flow patterns. Therefore, the predicted values by using the proposed model for the transition of flow patterns agree well with the experimental data. It is noteworthy that this model is only based on our experimental data, without comparison with others in the literature. Thus, maybe our model is lack of universality at this stage. However, our aim is not to claim that this model is better than previous ones, as the experimental data on the effects of liquid physical properties on the flow patterns in the literature are still rare. We also note that our model is similar to that developed by Zhang et al. [26], as except for the aspect ratio of the channel, other parameters are included in both models. Furthermore, our model seems to be strongly depend on the viscosity ratio of both phases, the aspect ratio and the dimensionless roughness of the channel, rather than the Weber number effects, which are clear from their exponents.

V. Conclusion

To conclude, the flow patterns of Newtonian/non-Newtonian fluids two-phase flow in rectangular micro channels are investigated. Four flow patterns are observed for cyclohexan/carboxyl methyl cellulose (CMC) solutions in T-shaped rectangular micro channels: slug flow, droplet flow, parallel flow and jet flow. It is found that the larger the concentration of CMC solutions and the smaller the micro channel, the wider of the regions are for the droplet flow and parallel flow. A corresponding model for the transition of flow patterns is established, based on several parameters such as the Weber number, the size of the micro channel, the physical properties of fluids, and the surface roughness. It is worth noting that further studies on dynamics of liquid–liquid two-phase flow containing non-Newtonian fluids, such as the pressure drop and mobility of droplets, will be presented in another article. This study is useful for further experimental and numerical investigations on multiphase flow in microfluidics and the design of micro reactors containing complex fluids.

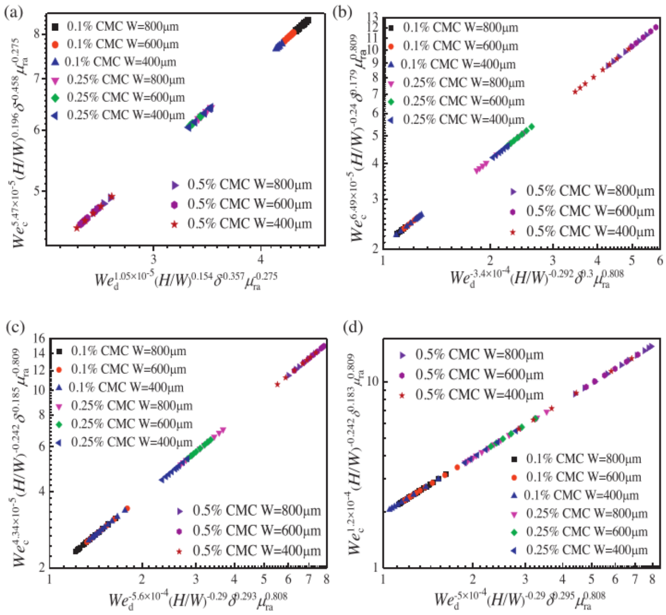

Fig. 8. The transitions for flow patterns of liquid–liquid two-phase flow in microchannels. (a) the transition from slug flow to droplet flow; (b) the transition from droplet flow to jet flow; (c) the transition from slug flow to jet flow; (d) the transition from jet flow to parallel flow.

References

[1] P. Nghe, E. Terriac, M. Schneider, Z.Z. Li, M. Cloitre, B. Abecassis, P. Tabeling, Microfluidics and complex fluids, Lab Chip 11 (2011) 788–794.

[2] F.J. Galindo-Rosales, M.A. Alves, M.S.N. Oliveira, Microdevices for extensional rheometry of low viscosity elastic liquids: a review, Microfluid. Nanofluid. 14 (2013) 1–19.

[3] A. Groisman, M. Enzelberger, S.R. Quake, Microfluidic memory and control devices, Science 300 (2003) 955–958.

[4] M.M. Denn, Fifty years of non-Newtonian fluid dynamics, AIChE J. 50 (2004) 2335–2345.

[5] X. Frank, J.-C. Charpentier, Y. Ma, N. Midoux, H.Z. Li, A multiscale approach for modeling bubbles rising in non-Newtonian fluids, Ind. Eng. Chem. Res. 51 (2011) 2084–2093.

[6] G.M. Whitesides, The origins and the future of microfluidics, Nature 442 (2006) 368–373.

[7] T.M. Squires, S.R. Quake, Microfluidics: fluid physics at the nanoliter scale, Rev. Mod. Phys. 77 (2005) 977–1026.

[8] R. Seemann, M. Brinkmann, T. Pfohl, S. Herminghaus, Droplet based microfluidics, Rep. Prog. Phys. 75 (2012) 016601.

[9] D. Mark, S. Haeberle, G. Roth, F. von Stetten, R. Zengerle, Microfluidic lab-on-achip platforms: requirements, characteristics and applications, Chem. Soc. Rev. 39 (2010) 1153–1182.

[10] C.-X. Zhao, A.P.J. Middelberg, Two-phase microfluidic flows, Chem. Eng. Sci. 66 (2011) 1394–1411.

[11] [L. Sang, Y. Hong, F. Wang, Investigation of viscosity effect on droplet formation in T-shaped microchannels by numerical and analytical methods, Microfluid. Nanofluid. 6 (2009) 621–635.

[12] [M.N. Kashid, L. Kiwi-Minsker, Microstructured reactors for multiphase reactions: state of the art, Ind. Eng. Chem. Res. 48 (2009) 6465–6485.

[13] T. Fu, Y. Ma, D. Funfschilling, H.Z. Li, Bubble formation in non-Newtonian fluids in a microfluidic T-junction, Chem. Eng. Process. Process Intensif. 50 (2011) 438–442.

[14] T. Fu, Y. Ma, D. Funfschilling, H.Z. Li, Gas–liquid flow stability and bubble formation in non-Newtonian fluids in microfluidic flow-focusing devices, Microfluid. Nanofluid. 10 (2011) 1135–1140 .

[15] Y. Zhao, G. Chen, Q. Yuan, Liquid–liquid two-phase mass transfer in the T-junction microchannels, AIChE J. 53 (2007) 3042–3053.

[16] K.V. Edmond, A.B. Schofield, M. Marquez, J.P. Rothstein, A.D. Dinsmore, Stable jets of viscoelastic fluids and self-assembled cylindrical capsules by hydrodynamic focusing, Langmuir 22 (2006) 9052–9056.

[17] M.N. Kashid, D.W. Agar, Hydrodynamics of liquid–liquid slug flow capillary microreactor: flow regimes, slug size and pressure drop, Chem. Eng. J. 131 (2007) 1–13.

[18] J.H. Xu, G.S. Luo, S.W. Li, G.G. Chen, Shear force induced monodisperse droplet formation in a microfluidic device by controlling wetting properties, Lab Chip 6 (2006) 131–136.

[19] T. Fu, Y. Ma, D. Funfschilling, C. Zhu, H.Z. Li, Breakup dynamics of slender bubbles in non-newtonian fluids in microfluidic flow-focusing devices, AIChE J. 58 (2012) 3560–3567.

[20] W. Lee, L.M. Walker, S.L. Anna, Competition between viscoelasticity and surfactant dynamics in flow focusing microfluidics, Macromol. Mater. Eng. 296 (2011) 203–213.

[21] S. Wang, J. Huang, K. He, J. Chen, Phase split of nitrogen/non-Newtonian fluid two-phase flow at a micro-T-junction, Int. J. Multiphase Flow 37 (2011) 1129–1134 .

[22] P.E. Arratia, L.A. Cramer, J.P. Gollub, D.J. Durian, The effects of polymer molecular weight on filament thinning and drop breakup in microchannels, New J. Phys. 11 (2009) 1150 06.

[23] R.B. Bird, P.J. Carreau, A nonlinear viscoelastic model for polymer solutions and melts—I, Chem. Eng. Sci. 23 (1968) 427–434.

[24] Z.C. Yang, Q.C. Bi, B. Liu, K.X. Huang, Nitrogen/non-Newtonian fluid two-phase upward flow in non-circular microchannels, Int. J. Multiphase Flow 36 (2010) 60–70.

[25] T. Al-Wahaibi, N. Yusuf, Y. Al-Wahaibi, A. Al-Ajmi, Experimental study on the transition between stratified and non-stratified horizontal oil–water flow, Int. J. Multiphase Flow 38 (2012) 126–135.

[26] T. Zhang, B. Cao, Y. Fan, Y. Gonthier, L. Luo, S. Wang, Gas–liquid flow in circular microchannel. Part I: Influence of liquid physical properties and channel diameter on flow patterns, Chem. Eng. Sci. 66 (2011) 5791–5803.

[27] M.K. Akbar, D.A. Plummer, S.M. Ghiaasiaan, On gas–liquid two-phase flow regimes in microchannels, Int. J. Multiphase Flow 29 (2003) 855–865.

[28] S. Waelchli, P.R. von Rohr, Two-phase flow characteristics in gas–liquid microreactors, Int. J. Multiphase Flow 32 (2006) 791–806.